An Experimental Study on Kinetics of Asphaltene Aggregation in a Microcapillary

Journal:	*Energy & Fuels*
Manuscript ID	ef-2017-011708
Manuscript Type:	Article
Date Submitted by the Author:	24-Apr-2017
Complete List of Authors:	Li, Xingxun; China University of Petroleum, Beijing, Department of Chemical Engineering Guo, Yunmei; China University of Petroleum, Beijing, Department of Chemical Engineering Boek, Edo; University of Cambridge, Department of Applied Mathematics and Theoretical Physics Guo, Xu-Qiang; China University of Petroleum, Beijing, College of Chemical Engineering

An Experimental Study on Kinetics of Asphaltene Aggregation in a Microcapillary

Xingxun Li[†], Yunmei Guo[†], Edo S. Boek[‡], Xuqiang Guo*[†]

[†]State Key Laboratory of Heavy Oil Processing, China University of Petroleum (Beijing), Beijing 102249, China

[‡]Department of Applied Mathematics and Theoretical Physics, University of Cambridge, Cambridge CB3 0WA, United Kingdom

Abstract

Asphaltentic and other polar organic compounds in crude oil form aggregates, precipitate, adhere to surfaces, block rock pores and severely alter the wetting characteristics of mineral surfaces within the reservoir, hindering oil recovery efficiency. Tremendous experimental efforts have been done to investigate asphaltene aggregation and precipitation from crude oil. Most of these works were carried out on planar mineral substrates or in bulk solution. However, not many direct measurements have been done in a small confined micro-sized pore. Examining asphaltene aggregation in a microcapillary might represent asphaltene deposition in reservoir pores better than the investigations on flat surfaces. Therefore, in this study we employ new methods to directly visualize the asphaltene aggregation process and investigate the kinetics of asphaltene aggregation in a microcapillary. The asphaltene aggregation behavior can be described by diffusion-limited aggregation (DLA) and

reaction-limited aggregation (RLA) models. Effects of concentration of asphaltene precipitant and temperature were investigated. The results indicate that the concentration of precipitant has a significant effect on the aggregation rate and aggregation mechanism. The asphaltene aggregation is faster at higher concentrations of precipitant. The kinetics of asphaltene aggregation at higher precipitant concentrations is predominantly controlled by DLA mechanism. The slow RLA mechanism mainly dominates the aggregation process at lower concentrations of precipitant. Elevated temperature leads to slow kinetics of asphaltene aggregation. The results were also compared with those measured on a flat surface in bulk solution in this study. At higher concentration of precipitant, the effect of confinement from the micro-sized capillary might lead to different asphaltene aggregation behaviors in a microcapillary from those in bulk solution.

1. Introduction

Crude oil is one of the most important fuel sources in our daily lives. Light oil has been readily recovered by primary and secondary recoveries methods, but large reserves of heavy oil still remain.[1, 2] Heavy oils often contain a significant amount of asphaltenes, which have been considered as the 'cholesterol' in crude oils. They can cause difficulties in recovering oil. Asphaltenes are commonly defined as a solubility class of crude oil components. Specifically, they are referred to as the fraction of crude oil which is insoluble in normal alkanes such as n-heptanes and n-pentane but

soluble in aromatics such as toluene and xylene.[3-5] The solubility of asphaltene or asphaltene-oil bulk phase equilibria is altered when temperature, composition or pressure of crude oil is changed during oil recovery and production.[6-9] The destabilized asphaltene will precipitate, aggregate and tend to create larger agglomerates from crude oil, and deposit in porous media, leading to reduced porosity and permeability, increased reservoir fluid viscosity, pore clogging, as well as surface wetting alteration.[10-12] This significantly damages reservoir formation. Therefore, it is crucial to build a comprehensive understanding on asphaltene destabilization (precipitation/aggregation) at a micro-pore scale. Prediction of the propensity of asphaltene to form aggregates and deposits is of great industrial interest. [13-17]

Numerous studies have been done on asphaltene aggregation, precipitation and deposition by coreflooding experiments, batch process, capillary tests and simulation.[18-29] For instance, Jafari Behbahani et al. investigated asphaltene adsorption in a sandstone core sample during CO_2 injection and reported significant reduction of porosity and permeability due to deposited asphaltene in core sample.[18] Boek's group studied the aggregation and deposition of colloidal asphaltene in capillary flow and estimated deposit thickness by experiments and simulations.[24-26] Gon and Fouchard used a custom-built asphaltene capillary deposition unit to evaluate the amount of asphaltene deposit inside the stainless-steel capillary unit under high temperature and pressure.[27] However, in most of these works, asphaltene destabilization and aggregation behaviors were only investigated by several

macroscopic parameters, such as pressure drop, porosity and permeability. They did not give direct visualization and analysis on asphaltene aggregation and precipitation behavior.

Recently, several works have been conducted to directly visualize the asphaltene aggregation and deposition.[30] Seifried et al. studied the kinetics of asphaltene aggregation as a function of various solvents and precipitants by using confocal laser-scanning microscopy and tracked the growth of asphaltene aggregates as a function of time.[31] Zanganeh et al. employed a novel visual cell to study the amount of deposited asphaltene and its size distribution by a high-resolution microscope and image processing technique.[32, 33] Mohammadi et al. indicated that asphaltene aggregates in light live oil were temperature-pressure fractal structures and revealed the significant effect of temperature on asphaltene aggregation by micro-visualization experiments.[34] In these recent works, aggregation and precipitation of asphaltene were studied on planar substrates in bulk solutions, but they may not provide insight in the asphaltene aggregation in porous media. As known, the direct measurement in a confined pore could represent the porous fluid phenomena better than those measured on flat substrates.[35, 36] In order to advance the asphaltene precipitation and aggregation in porous media, we developed a new method to directly visualize the growth of asphaltene aggregates and measure the kinetics of asphaltene aggregation in a micro-sized pore. The effects of concentration of asphaltene precipitant and temperature were studied.

2. Experimental Section

2.1 Materials

The crude oil used in this study was obtained from Venezuela. It has an n-heptane asphaltene weight content of around 14% with a high potential of asphaltene formation. The kinetic viscosity was 1000 mPa•s at 50 ℃ and the density was 0.975 g/cm^3. Toluene (Beijing Shiji, 99.5%) was used as solvent. n-heptane (Nankai Rungong, 98.5%) was used as asphaltene precipitant, which is a well-characterized asphaltene precipitant. Square borosilicate glass microcapillaries (Beijing Zhong Cheng Quartz Glass) with open ends were used in experiments. To clearly visualize the growth of asphaltene aggregates, the capillaries are highly transparent and have a precise optical path length. Each capillary used is 20 mm long and 100 μm wide with a volume of 0.2 μL.

2.2 Methods

In order to initiate the asphaltene precipitation and study the kinetics of asphaltene aggregation, diluted oils, which are precipitant (n-heptane)-solvent (toluene)-crude oil mixtures, were used in this study. 1 ml of crude oil was diluted by 40 ml of mixture of n-heptane and toluene. The asphaltene precipitation onset (APO) was first roughly detected by filtration method using gravimetric analysis at ambient conditions. The APO is approximately at 50 vol% n-heptane. Four concentrations of asphaltene precipitant were used in this study, which are 50 vol%, 60 vol%, 70 vol% and 80 vol%

n-heptane. They are close to and above the asphaltene precipitation onset. As shown in Figure 1, the diluted oil was placed on a Constant-temperature Magnetic Stirrer (B11-3, Sile Instrument). The diluted oil was continuously stirred by magnetic stir bars in a beaker with a constant stirring speed of 300 r/min. A hot water bath located on the heat pad of the constant-temperature magnetic stirrer was used to maintain an elevated temperature for the diluted oil (Figure 1). Three temperatures were investigated in this study, which are 20℃，40℃ and 70℃.

Before measurements, general cleaning methods were adopted to clean the capillaries.[35-38] The capillaries were first washed by using sodium hydroxide solution and nitric acid solution, then soaked in an acetone bath, and finally thoroughly rinsed with deionized water for 1 hour. A few minutes prior to each test, the capillaries were dried in an ash-proof condition. All the capillaries were handled carefully with clean tweezers to avoid capillary interior contamination.

The glass microcapillaries were aged in the diluted oil for various times (Figure 1). The aging time ranged from t=0 min to t=300 min. To image the asphaltene aggregates in a microcapillary, the glass microcapillary was then taken out of the diluted oil and immediately placed under a microscope for observation and image capturing. The microscope (Changrong S-T) was equipped with a high-speed digital camera (Aptina-LV500). The microscope stage was movable, allowing for capturing images along the length of the capillary in order to take the images of asphaltene

aggregates at different locations of capillary. To obtain statistically reliable results, about 10~15 images were taken along for per capillary at various locations. In order to measure the asphaltene aggregation in bulk on a planar substrate, a small drop of sample was placed between a glass slide and a cover sheet. A drop of immersion oil was placed onto the cover sheet to avoid the refraction of light and contribute to observation under microscope. The size and number of asphaltene aggregates were measured and analyzed with Image-Pro Plus 6.0 and Image View software.

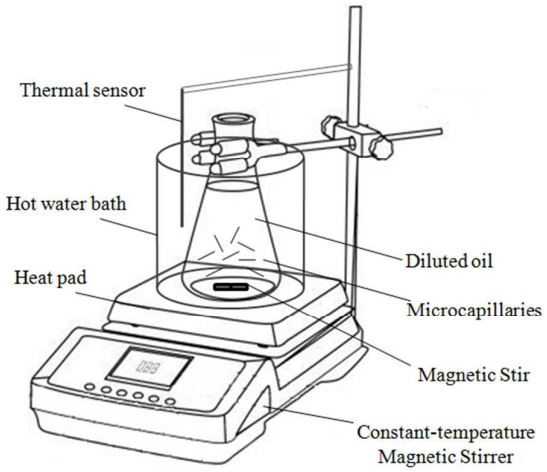

Figure 1 Microcapillaries aged in diluted oil

Hildebrand solubility parameter (δ) is used here to describe the degree of solubility of synthetic oil (Equation 1),[39]

$$\delta = \sqrt{\frac{\Delta H - RT}{V}} \quad (1)$$

where ΔH is heat of vaporization, R is gas constant, T is temperature and V is molar volume.

For nonpolar species, to obtain Hildebrand solubility parameter (δ), a simplified and empirical correlation between solubility parameter and refractive index (RI) can be gained linearly at ambient temperature,[40]

$$\delta(MPa^{1/2})=52.042F_{RI}+2.904 \quad (2)$$

where

$$F_{RI}=(n^2-1)/(n^2+2) \quad (3)$$

where n is the RI.

Hildebrand solubility parameter (δ) for the mixture was obtained from the volume fractions of the components i,[31, 41, 42]

$$\delta_{mixture} = \sum \delta_i \varphi_i \quad (4)$$

where φ is the volume fraction of the component i.

Refractive index (RI) of each component was measured by a refractometer (Rudolph, J257). The Hildebrand solubility parameters (δ) of diluted crude oils were calculated by equations (2-4). They are 16.736 $MPa^{0.5}$, 16.451 $MPa^{0.5}$, 16.166 $MPa^{0.5}$ and 15.881 $MPa^{0.5}$ for 50 vol%, 60 vol%, 70 vol% and 80 vol% heptane-toluene-oil mixtures, respectively.

Two possible models of colloid particle aggregation were predicted by classic DLVO theory, which are diffusion-limited aggregation (DLA) and reaction-limited aggregation (RLA).[43, 44] They have been recently used to describe the asphaltene aggregation process in crude oil.[11, 31, 45] The diffusion-limited aggregation (DLA) model describes fast aggregation governed by colloidal particle diffusion; any contact between asphaltene particles causes coagulation. On the other hand, not every contact of particles leads to their coupling in the reaction-limited aggregation (RLA) model; a large number of collisions are required before particles form aggregates. The difference between these two models is the way that particles stick together. [44]

Diffusion-limited aggregation (DLA) describes the particle growth by equation (5),[30]

$$R = R_0 \left(1 + \frac{t}{\tau_D}\right)^{1/d_f} \quad (5)$$

While, reaction-limited aggregation (RLA) describes the particle growth by equation (6) ,[30]

$$R = R_0 \exp(t/\tau_R d_f) \quad (6)$$

Where R is the mean radius of the aggregates, R_0 is the initial radius, t is the flocculation time, τ_D is the diffusion time,τ_R is the reaction time, and d_f is the fractal dimension. d_f is different for DLA and RLA. It relates to the aggregate size

and number of aggregates.[46, 47]

4. Results and Discussion

4.1 Asphaltene Aggregates in a Glass Capillary

To study the kinetics of asphaltene aggregation in porous media, the asphaltene aggregation process in a highly transparent glass microcapillary was investigated at the micro scale. n-heptane was used as precipitant and toluene served as oil solvent. Figure 2 shows the microscopic images of asphaltene aggregates precipitated with 60 vol% n-heptane at various flocculation times in a microcapillary. The size, size distribution and number of asphaltene aggregates can be analyzed from these high-resolution microscopic images.

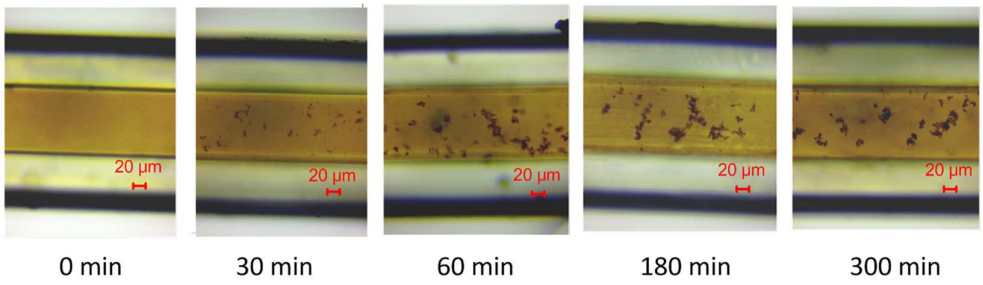

Figure 2 Microscopic images of the asphaltene aggregates in the crude oil precipitated with 60 vol% of n-heptane at various flocculation times (0 min, 30 min, 60 min, 180 min and 300 min)

Figure 3 shows the average diameter of asphaltene aggregates for 60 vol%

n-heptane-toluene-oil system in a glass capillary as a function of flocculation time from 0 to 300 min. As shown in Figure 3, at t=0 min, the initial asphaltene aggregates are with small sizes of around 2.2 μm. The size of asphaltene aggregates increases significantly over the flocculation time from 0 to 60 min due to the aggregation of the existing flocs. The average diameters of asphaltene aggregates are around 3.9 μm and 6.4 μm at t=30 min and t=60 min, respectively. However, after t=60 min, aggregate size does not increase with flocculation time. The average aggregate diameter stays around 5.5 μm due to the sedimentation of asphaltene aggregates.[31]

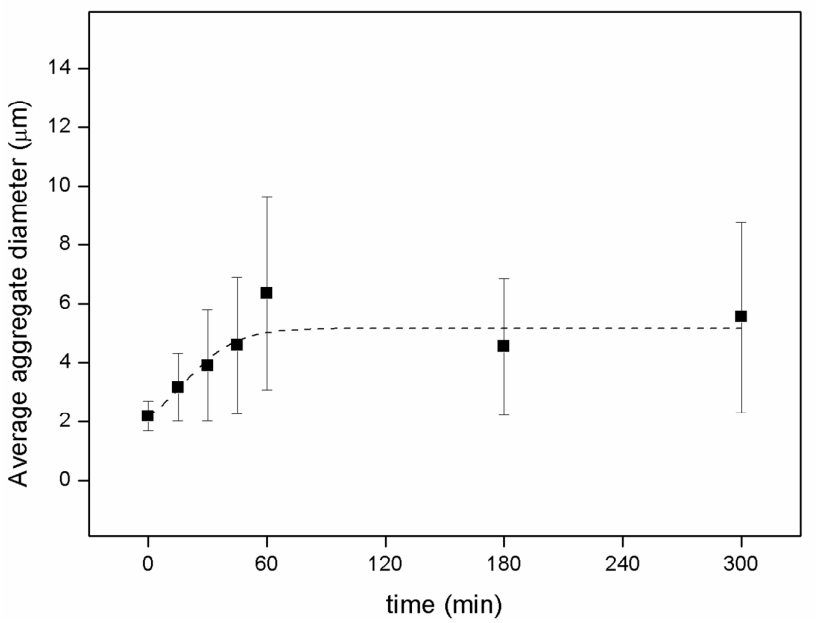

Figure 3 Average diameter of asphaltene aggregates as a function of flocculation time.

4.2 Effect of Concentration of Asphaltene Precipitant on Diameter and Size Distribution of Aggregates

The effect of concentration of asphaltene precipitant on the kinetics of asphaltene aggregation in a microcapillary at ambient temperature was investigated in this study. Four concentrations of asphaltene precipitant are investigated, which are 50 vol%，60 vol%，70 vol% and 80 vol% n-heptane. The microscopic images of asphaltene aggregates at these four different concentrations in a microcapillary at flocculation time of 30 min are shown in Figure 4. Figure 5 presents the average diameter of asphaltene aggregates as a function of flocculation time in heptane-toluene-oil systems with different concentrations of n-heptane. The results indicate the significant effect of the concentration of asphaltene precipitant on asphaltene aggregate growth in a microcapillary (Figure 5). For example, when 70 vol% n-heptane is used, at t=0 min, the initial asphaltene aggregate size is around 5 μm, which is remarkably larger than that for 60 vol% n-heptane-toluene-oil system at t=0 min. As flocculation time increases, the average diameter of asphaltene aggregates for 70 vol% n-heptane-toluene-oil system increases in a faster fashion than that for 60 vol% n-heptane-toluene-oil system before the flocculation time reaches t=60 min. At t=60 min, the average diameter of aggregates reaches a maximum around 10 μm. When the 80 vol% n-heptane is used, the size of asphaltene aggregates increases with the flocculation time most significantly at early time. The average diameter of asphaltene aggregates increases from around 5 μm to 21 μm from t=0 min to t=45 min. After

t=45 min, the asphaltene particles stop aggregation because aggregates start to sediment.

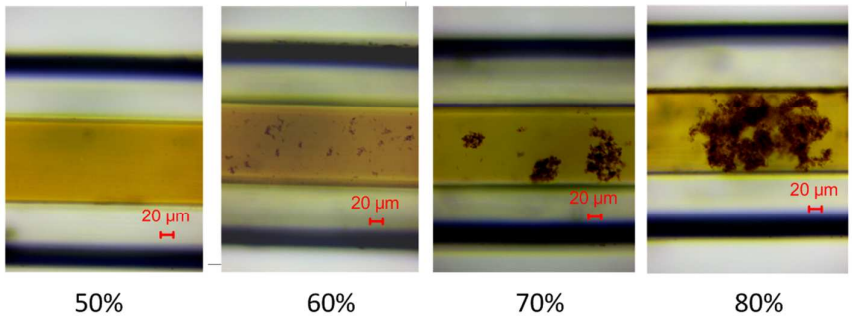

Figure 4 Microscopic images of the asphaltene aggregates in the crude oil precipitated with 50/60/70/80vol% of n-heptane at flocculation time of 30 min

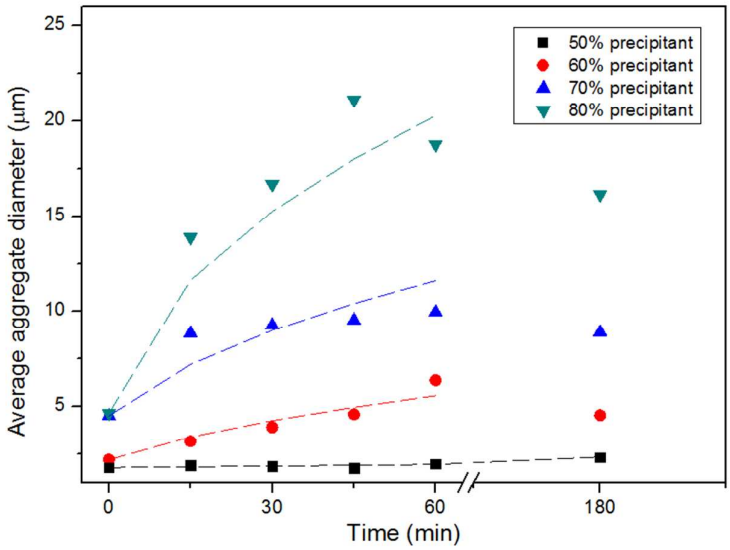

Figure 5 Average asphaltene diameter as a function of flocculation time with various concentrations of precipitants (50 vol%，60 vol%，70 vol% and 80 vol% n-heptane)

As shown in Figure 5, larger asphaltene aggregate sizes are obtained for higher concentrations of n-heptane when sedimentation starts. This might be caused by the viscosity of the suspension increasing with higher concentrations of n-heptane based on Stokes' law. The kinematic viscosities of 60 vol%, 70% vol% and 80% vol% n-heptane-toluene-oil mixtures were measured using a glass capillary viscometer (ISO/3105-76). The values are 0.6703, 0.7973 and 0.8802 mm^2/s, respectively. The viscosity of mixtures increases with increasing heptane concentration, presumably due to the increased asphaltene content in the suspension rather than heptane or toluene content. This is also confirmed by other studies.[48, 49] Figure 5 indicates an increase in particle size of about a factor of over 3, but the viscosity only increases by a factor of (0.88/0.67 ≈ 1.3) from the 60 vol% to 80 vol% n-heptane. Stokes' law can be used to determine the size of sedimenting aggregates based on the fluid viscosity (Equation 7).

$$d_p = \left(\frac{18u}{g(\rho_p - \rho)}\right)^{0.5} \mu^{0.5} \quad (7)$$

where d_p is particle size, ρ_p and ρ are the mass densities of particle and fluid, u is sedimentation velocity and μ is fluid viscosity.

Assuming densities and sedimentation velocity remain constant, the particle size of sedimenting aggregates should increase with the square root of viscosity as shown in Figure 6 (a). Figure 6 (a) shows the aggregate size of sedimentation as a function of

viscosity using double logarithmic axes for scaling purposes. We observe that the scaling exponent of the critical experimental aggregate size for sedimentation as a function of viscosity is approximately 4.5. This value is much larger that the Stokes' law exponent of 0.5. This implies that there are factors other than the viscosity which also affect the aggregate size of sedimentation. The reasons might be complex and need to be assessed and confirmed in further studies. In addition, our experimental data on sedimentation size is compared with the data from Seifried and Boek,[31] as shown in Figure 6 (b). They give similar trends with the same slopes but different magnitudes. The difference could be caused by different crude oils and experimental methods.

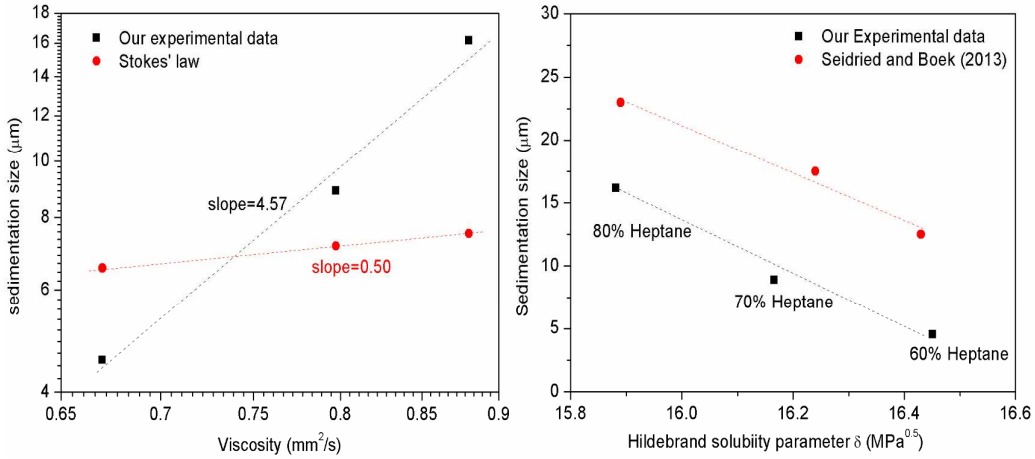

(a) (b)

Figure 6 (a) The critical aggregate size of sedimentation as a function of viscosity using double logarithmic scaling; (b) The aggregate size of sedimentation as a function of Hildebrand solubility parameter for various concentrations of precipitants (60 vol%，70 vol% and 80 vol% n-heptane) in diluted crude oil (Hildebrand solubility

parameters (δ) of diluted crude oils are calculated by Equations (2-4) in Experimental section).

The 50 vol% of n-heptane-toluene-oil system close to the asphaltene precipitation onset (APO) was also investigated. As shown in Figure 5, the asphaltene aggregation for 50 vol% of n-heptane-toluene-oil mixtures is much slower than those for the other three mixtures with higher precipitant concentrations. The diameter of asphaltene aggregation increases with the flocculation time by only around 0.6 μm from t=0 min to 180 min. At t=180 min, the average diameter of asphaltene aggregates is around 2.3 μm; the maximum diameter of asphaltene aggregates was only 5.5μm. Near the onset, only small asphaltene particle appears.

Two models have been commonly applied to describe irreversible particle aggregation process, which are diffusion-limited aggregation (DLA) (Equation 1) and reaction-limited aggregation (RLA) (Equation 2).[43, 44] In this study, these two models are applied to describe and explain our experimental data of asphaltene aggregate growth in a microcapillary. In Figure 5, the experimental data of aggregate size versus flocculation time is fitted with Equation 1 (DLA) and Equation 2 (RLA). The dotted lines in Figure 5 represent the fit functions. When 70 vol% and 80 vol% n-heptane are used, the experimental data can be fitted to DLA before the sedimentation of asphaltene aggregation starts. In DLA, every collision results in sticking of particles to one another and generating larger aggregates, which might cause fast particle

aggregation.[46] Figure 5 indicates that the kinetics of asphaltene aggregation for the 50 vol% and 60 vol% n-heptane-toluene-crude oil systems is different from those for the other two systems with higher precipitant concentrations. The slow reaction-limited aggregation (RLA) mainly dominates the kinetics of asphaltene aggregation. A large number of collisions are required before two particles stick to one another. This is against fast aggregation. The experimental data for 50 vol% and 60 vol% n-heptane-toluene-crude oil systems are fitted to RLA model (Figure 5).

In DLA and RLA models (Equation 1 and 2), the diffusion time (τ_D), reaction time (τ_R) and fractal dimensionality (d_f) are adjusting parameters, which are shown in Table 1.Table 1 indicates that the fractal dimensionality (d_f) increases with the concentration of precipitant. The higher value of fractal dimensionality (d_f) implies the more dense and compact of asphaltene aggregates. The fractal dimensionality (d_f) obtained in this study is in agreement with the range of fractal dimensionality in previous studied (Table 1). For the RLA-dominated 50 and 60 vol% n-heptane-toluene-oil systems, the reaction times (τ_R) are much longer than the diffusion times (τ_D) for the DLA-controlled 70 and 80 vol% n-heptane-toluene-crude oil systems. For the DLA-dominated 70 and 80 vol% n-heptane-toluene-crude oil systems, the diffusion time (τ_D) becomes shorter as the concentration of precipitant increases. The fitting parameters (τ_D, τ_R and d_f) are also compared with the values from previous studies. Similar results have been reported in previous studies as shown in Table 1.[31, 34, 46]

Table 1 Fitting parameters in DLA and RLA

Concentration of precipitant	d_f	Characteristic time (min)	
		τ_D	τ_R
50%	1.82	—	360
60%	2.10	—	26
70%	2.40	6	—
80%	2.70	1.1	—
Ashoori et al. [46]	1.53~2.00	0.93~1.3	18.6~28.2
Seifried and Boek [31]	1.50~3.80	1.5~3.8	—
Mohammadi et al. [34]	1.64~2.00	—	—

Our experimental data is also compared with recent relevant studies on kinetics of asphaltene aggregation reported in the literature,[30, 31] as shown in Figure 7. We review and discuss two works from Hung et al. and Seifried and Boek. Both of these two works reported the asphaltene aggregation process for the n-heptane-toluene-oil system, which was similar to the system used in this study. Experimental methods and crude oil we used differ from those in these studies. The crude oil used in Seifried and Boek's study was from Shell, with a high n-heptane asphaltene content of 18.8 wt%, a density of 0.983 g/cm^3 and a kinematic viscosity of 20020 mm^2/s at 40 ℃.[31] Hung et al. used Boscan crude oil (11^{o}API, 17 wt% asphaltene).[30] The colloid structural evolution and aggregation process of asphaltene are indeed different from the other crude oils. These thus might not give a perfect comparison. However, we still think that it is worth to compare them to evaluate the kinetics of asphaltene aggregation. Hung et al. studied the kinetics of asphaltenes in Boscan crude oil at 66 vol% and 88 vol% of n-heptane. They found that the growth of the asphaltene aggregates was

faster at initial stage and increased until they reached a maximum size. The growth of asphaltene aggregates at high concentration of n-heptane is faster than that at low concentration of n-heptane. These findings are in good agreement with our results. In addition, our results are also compared with the data from Seifried and Boek. The trend of kinetics of asphaltene aggregation they obtained was similar with the one at high n-heptane concentration in this study (Figure 7).

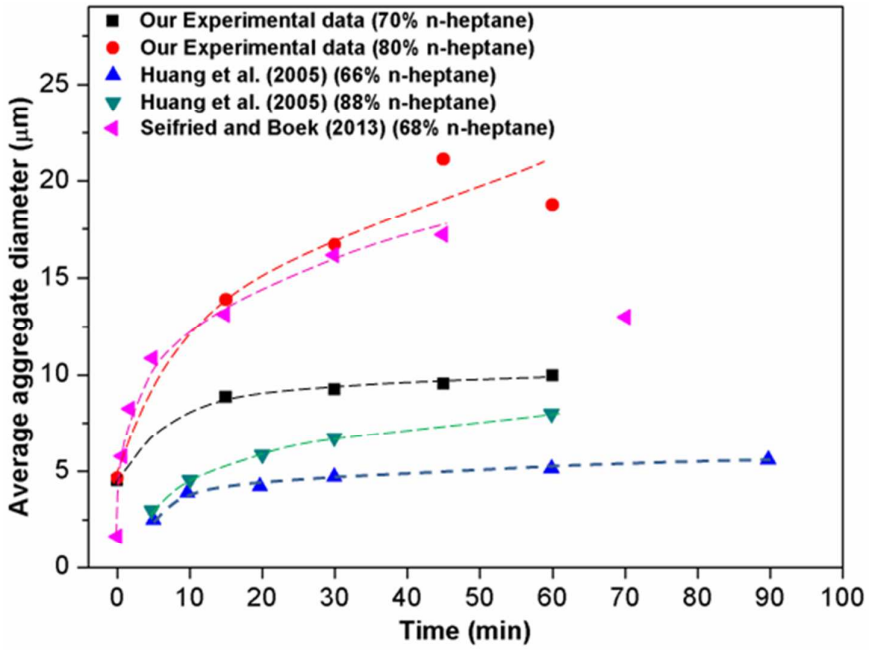

Figure 7 Comparison of our experimental data with values reported in literature[30, 31]

The size distributions of asphaltene aggregates at various flocculation times are also investigated in this study. Table 2 shows the size distributions of asphaltene aggregates obtained in 50/60/70/80 vol% n-heptane-toluene-oil mixtures at flocculation times of t=0 min, 30 min and 60 min. For the 50 vol% n-heptane-toluene-oil system, the diameters of asphaltene aggregates are within a very

narrow size range, which is only from 1.0 μm to 4.5 μm. The sizes of asphaltene aggregates mainly range from 1.5 μm to 2.5 μm. The size distribution becomes slightly broader as flocculation time increases. This might imply the slow kinetics of aggregation or reaction-limited control of the aggregation process. The concentration of precipitant significantly affects the size distribution of asphaltene aggregate. The size distribution becomes broader and multimodal as the concentration of precipitant increases (Table 2). For instance, when 60 vol% n-heptane is used, at a flocculation time of t=30 min, the aggregate size ranges from 1.5 μm to 22.5 μm. A unimodal aggregate size distribution is observed. The aggregation size mainly ranges from 1.5 μm to 7.5 μm, which accounts for 92% of the total number of aggregates. When the concentration of precipitant increases to 80% at a flocculation time of t=30 min, a wider aggregate size range is obtained, which is from 1.5 μm to 89.5 μm. The size distribution has a degree of polydispersity. The effect of flocculation time on aggregate size distribution is also indicated in Table 2. For instance, for the 60 vol% n-heptane-toluene-oil system, the aggregation occurs over a very broad size range up to 46.5 μm at flocculation time of t=60 min, compared with the narrow aggregate size range from 0.75 μm to 6.0 μm at flocculation time of t=0 min.

Table 2 Size distribution of asphaltene aggregates of 50/60/70/80 vol% n-heptane-toluene-crude oil mixtures at different flocculation times

Heptane Concentration (Vol%)	Flocculation time		
	0 min	**30 min**	**60 min**
50%	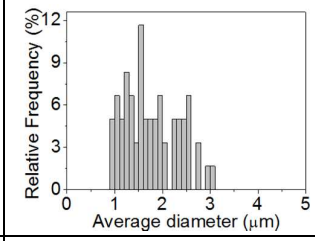	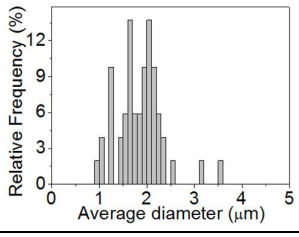	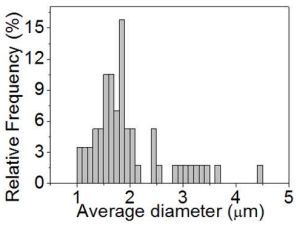
60%	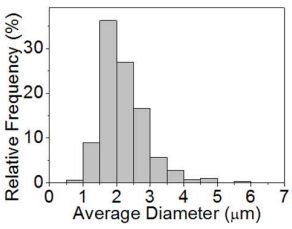	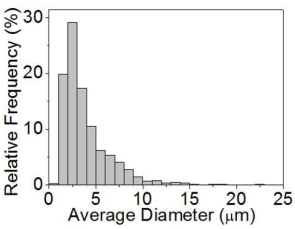	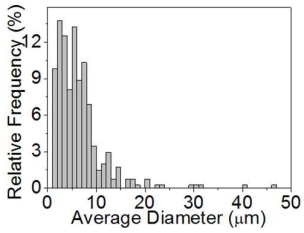
70%	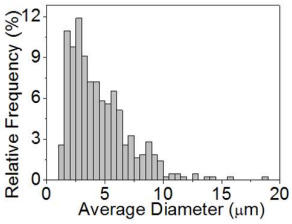	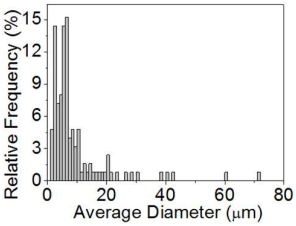	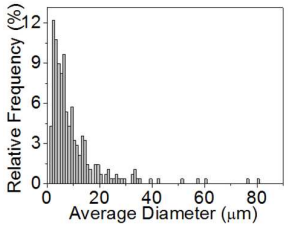
80%	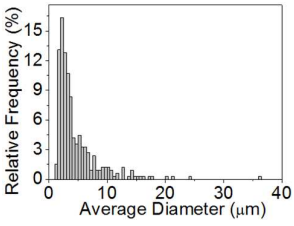	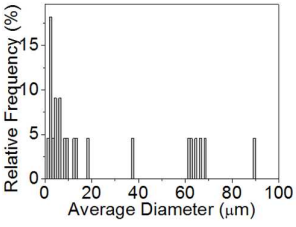	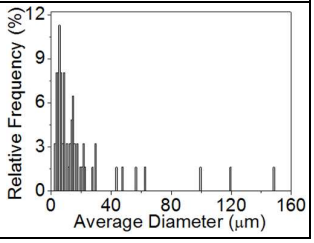

In addition, the number of asphaltene aggregates is also studied as a function of flocculation time. For instance, Figure 8 (a) and (b) shows the evolution of the number of particles of asphaltene as a function of flocculation time from 0 to 180 min, for 80 vol% and 50 vol% n-heptane-toluene-crude oil mixtures, respectively. For 80 vol% n-heptane-toluene-crude oil mixture, the number of small asphaltene aggregates

decreases with time because of the formation of larger clusters or flocs of asphaltene particles and the aggregates becomes larger. For instance, at a flocculation time of t=30 min, the average number of aggregates is around 6 and the size of largest aggregate is 92.6 μm. They almost completely block the micro-sized pore, as shown in Figure 4. The asphaltene aggregation process is controlled by the diffusion of aggregates. Every contact of the floc particles causes their coupling. On the other hand, for 50 vol% n-heptane-toluene-crude oil mixtures, the number of aggregates does not diminish as time increases. The number of aggregates increases from around 10 at initial stage to 45 at flocculation time of t=180 min. This process is predominantly determined by the slow reaction-limited aggregation (RLA) mechanism.

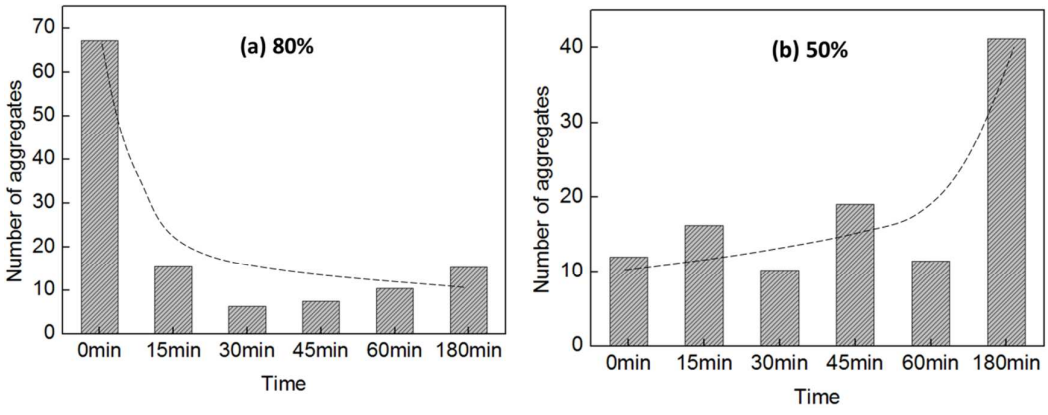

Figure 8 Number of asphaltene aggregates as a function of flocculation time for (a) 80 vol% n-heptane and (b) 50 vol% n-heptane

4.3 Effect of Temperature on Diameter and Size Distribution of Aggregates

In this section, the effect of temperature on the asphaltene aggregation in a microcapillary is investigated. Figure 9 shows the average diameter of asphaltene aggregates for 60 vol% n-heptane-toluene-oil mixture at 20℃，40℃ and 70℃. The average diameters of asphaltene aggregates increase exponentially with time which can be fitted to the RLA model (Equation 2). The fitting parameters, fractal dimensionality(d_f) and reaction time(τ_R), are summarized in Table 3. The fractal dimensionality decreases and reaction time increases as temperature is elevated. As depicted in Figure 9, the average diameter of asphaltene aggregates at 20℃ is significantly larger than those at 40℃ and 70℃. The rates of asphaltene aggregation at 40℃ and 70℃ are much slower than that at 20℃. At initial stage, the aggregation sizes at 40℃ are similar to the ones at 70℃. After a flocculation time of t=15 min, the asphaltene aggregation at 40℃ is slightly faster than that at 70℃. The size distributions of aggregates at these three temperatures are also studied. Table 4 shows the size distributions obtained in a 60 vol% n-heptane-toluene-oil mixture at 20℃，40℃ and 70℃ at flocculation times of t=0 min, 30 min and 60 min. It can be seen that the size distribution becomes broader as temperature decreases. For example, at a flocculation time of t=60 min, the aggregate size mainly ranges from 0.5 to 46.5μm, 1.1 to 9.3 μm and 1.1 to 5.1 μm at 20 ℃，40 ℃ and 70 ℃, respectively. Thus, it can be concluded that elevated temperature makes the oil a better solvent and slows the rate of aggregation. Maqbool et al. studied the effect of temperature on aggregation

rate and reported that raising the temperature reduced the amount of asphaltene aggregation,[50] which is consistent with our findings.

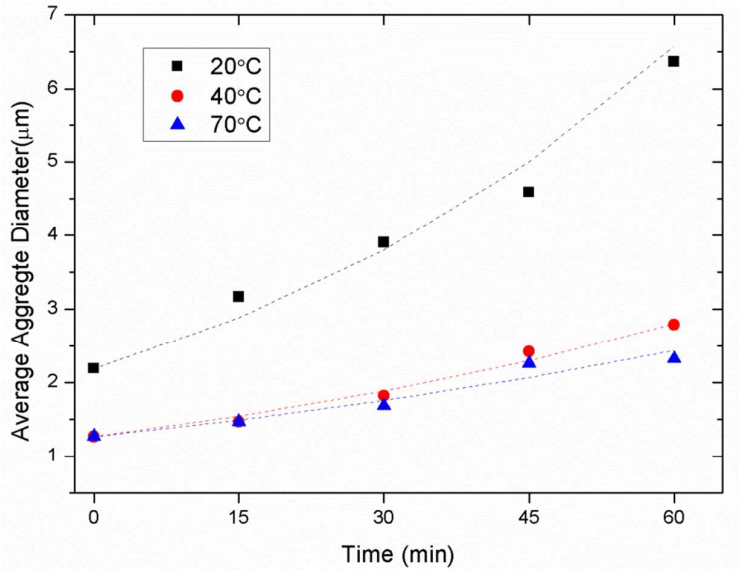

Figure 9 Average asphaltene diameter as a function of flocculation time at 20℃, 40℃ and 70℃

Table 3 Fitting parameters in RLA

Concentration of precipitant	d_f	τ_R(min)
20℃	2.1	26
40℃	1.89	40
70℃	1.83	50

Table 4 Size distribution of asphaltene aggregates of 60 vol% n-heptane-toluene-crude oil mixtures at different flocculation times

Tempera -ture	Flocculation time		
	0 min	**30 min**	**60 min**
20℃	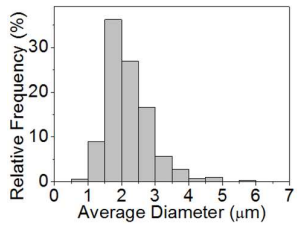	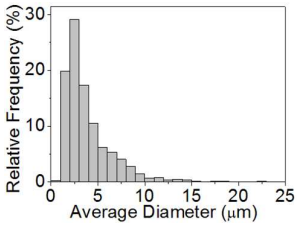	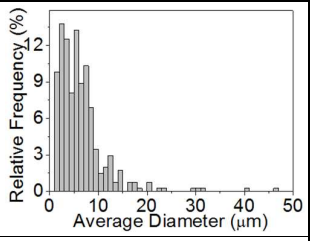
40℃	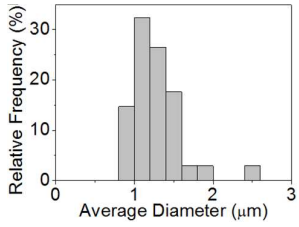	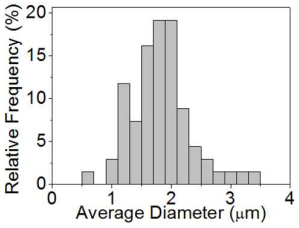	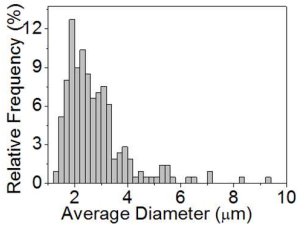
70℃	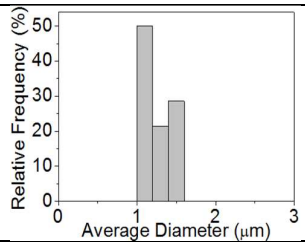	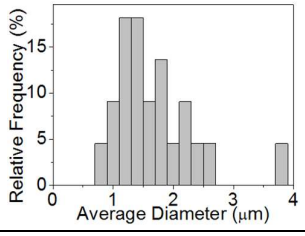	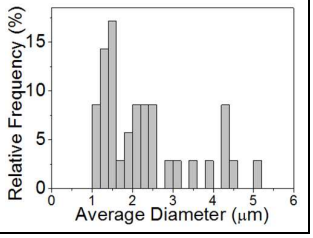

4.4 Asphaltene Aggregation on a Planar Substrate in Bulk Solution

The kinetics of the asphaltene aggregation in bulk solution on a planar substrate at ambient condition is also investigated in this study. Figure 10 (a) and (b) show the average size of asphaltene aggregates as a function of flocculation time in bulk solution on a planar substrate for 60 vol % and 80 vol % of n-heptane-toluene-crude oil mixtures, respectively. The results are compared with the kinetics of aggregate growth in a confined microcapillary (Figure 10).

In Figure 10 (a), the size of asphaltene aggregate increases with the flocculation time in bulk solution. The aggregate size increases almost linearly over time in bulk solution on a planar substrate. It is difficult to be fitted well by either DLA or RLA. This might be an indication of the crossover between diffusion-limited aggregation (DLA) and reaction-limited aggregation (RLA). Seifried and Boek studied the kinetics of asphaltene aggregation on a flat glass slide by using the similar precipitant-solvent-oil system we used in this paper.[31] They obtained similar findings.[31] It can be seen from Figure 10 (a) that the size difference of asphaltene aggregate in bulk solution on a planar substrate and in a microcapillary is insignificant at 60 vol % n-heptane. The size difference of aggregate is around 0.2~0.8μm.

However, at higher concentration of n-heptane (80 vol%), the asphaltene aggregation rate in a microcapillary is significantly faster than that in bulk solution on a planar substrate. After flocculation time of t=15 min, the aggregate sizes in a microcapillary are larger than those in bulk solution on a planar substrate at 80 vol% n-heptane, by around 2~10 μm. Buckley also observed the difference of asphaltene aggregation kinetics between in bulk solution and in a capillary, but did not give quantitative analysis. The difference could be explained by the effect of confinement of capillary tube or various asphaltene-surface interactions.[11] Other recent studies also reveal the effect of confinement on the phase behavior of fluids.[51-53] Luo et al. proposed that phase behavior in confined geometries was significantly altered from the bulk.[53]

However, this change of phase behaviour is complex and needs to be assessed and confirmed further.[11]

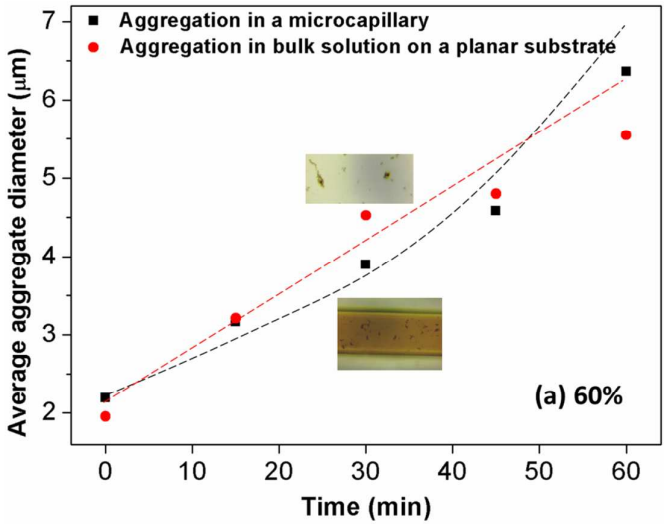

(a)

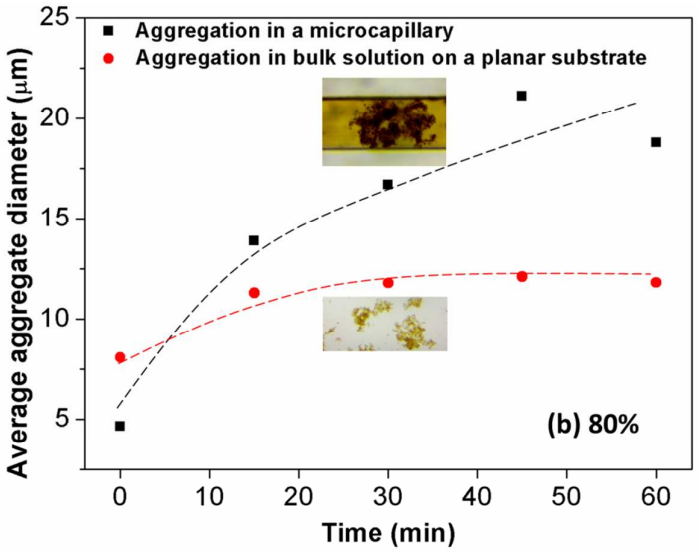

(b)

Figure 10 Comparison of kinetics of asphaltene aggregation in a microcapillary with on flat slide in bulk solution (a) 60 vol% n-heptane-toluene-crude oil mixtures; (b) 80 vol% n-heptane-toluene-crude oil mixtures

5. Conclusions

We present a new method for direct pore-scale visualization of the growth of asphaltene aggregates and measurement of the kinetics of asphaltene aggregation in a microcapillary instead of conventional methods. The experimental data was described by DLA and RLA models. The results obtained in a micro-sized pore might represent the asphaltene aggregation process in porous media better than those measured in bulk solution.

The size and size distribution of asphaltene aggregates as a function of flocculation time in a microcapillary were studied. As flocculation time increases, the size of aggregates becomes larger until sedimentation occurs, and size distribution becomes wider.

The effects of precipitant concentration and temperature on the kinetics of asphaltene aggregation in a microcapillary were investigated. The concentration of precipitant not only affects the aggregation rate but also the aggregation mechanism. The asphaltene aggregates more rapidly at higher concentration of precipitant. At lower concentrations (50 and 60 vol% n-heptane) of precipitants, the slow RLA mechanism mainly dominates the aggregation process. The kinetics of asphaltene aggregation at higher precipitant concentrations (70 and 80 vol% n-heptane) is predominantly controlled by the DLA mechanism. Effect of temperature on kinetics of asphaltene aggregation is significant. Slow asphaltene aggregation is detected at elevated

temperatures. We compared our results with values in the recent literature and obtain good agreement.

The results were also compared with those measured on a planar substrate in bulk solution in this study. At the lower concentration of precipitant, the difference of asphaltene aggregation kinetics between in bulk solution and in a capillary is not significant. However, at higher concentration of precipitant, the growth of asphaltene aggregates in a confined microcapillary is faster than that in bulk solution on a planar substrate. The confinement of micro-sized capillary might cause different aggregation behavior in a microcapillary from that in bulk solution, but this still needs to be investigated further and confirmed in our future work.

Acknowledgements

This work was supported by Science Foundation of China University of Petroleum, Beijing (2462016YJRC005) and supported by Science Foundation of China University of Petroleum，Beijing (2462017BJB05).

References

(1) Nobakht, M.; Moghadam, S.; Gu, Y., *Fluid Phase Equilibria* **2008**, *265,* 94-103.

(2) Moghadam, S.; Nobakht, M.; Gu, Y., *Journal of Petroleum Science and*

Engineering **2009**, *65,* 93-104.

(3) Kazemzadeh, Y.; Malayeri, M. R.; Riazi, M.; Parsaei, R., *Journal of Natural Gas Science and Engineering* **2015**, *22,* 227-234.

(4) Doryani, H.; Kazemzadeh, Y.; Parsaei, R.; Malayeri, M. R.; Riazi, M., *Journal of Natural Gas Science and Engineering* **2015**, *26,* 538-548.

(5) Vargas, F. M.; Gonzalez, D. L.; Creek, J. L.; Wang, J.; Buckley, J.; Hirasaki, G. J.; Chapman, W. G., *Energy & Fuels* **2009**, *23,* 1147-1154.

(6) Alboudwarej, H.; Akbarzadeh, K.; Beck, J.; Svrcek, W. Y.; Yarranton, H. W., *AIChE Journal* **2003**, *49,* 2948-2956.

(7) Hammami, A.; Phelps, C. H.; Monger-McClure, T.; Little, T. M., *Energy & Fuels* **2000**, *14,* 14-18.

(8) Groenzin, H.; Mullins, O. C., *The Journal of Physical Chemistry A* **1999**, *103,* 11237-11245.

(9) Speight, J., G., *Oil & Gas Science and Technology - Rev. IFP* **2004**, *59,* 467-477.

(10) Mullins, O. C.; Sabbah, H.; Eyssautier, J.; Pomerantz, A. E.; Barré, L.; Andrews, A. B.; Ruiz-Morales, Y.; Mostowfi, F.; McFarlane, R.; Goual, L.; Lepkowicz, R.; Cooper, T.; Orbulescu, J.; Leblanc, R. M.; Edwards, J.; Zare, R. N., *Energy & Fuels* **2012**, *26,* 3986-4003.

(11) Buckley, J. S., *Energy & Fuels* **2012**, *26,* 4086-4090.

(12) Jafari Behbahani, T.; Ghotbi, C.; Taghikhani, V.; Shahrabadi, A., *Energy & Fuels* **2013**, *27,* 622-639.

(13) Vilas Bôas Fávero, C.; Maqbool, T.; Hoepfner, M.; Haji-Akbari, N.; Fogler, H. S.,

Advances in Colloid and Interface Science.

(14) Durand, E.; Clemancey, M.; Lancelin, J.-M.; Verstraete, J.; Espinat, D.; Quoineaud, A.-A., *Energy & Fuels* **2010**, *24,* 1051-1062.

(15) Angle, C. W.; Long, Y.; Hamza, H.; Lue, L., *Fuel* **2006**, *85,* 492-506.

(16) Chandio, Z. A.; M, R.; Mukhtar, H. B., *Chemical Engineering Research and Design* **2015**, *94,* 573-583.

(17) Painter, P.; Veytsman, B.; Youtcheff, J., *Energy & Fuels* **2015**, *29,* 2951-2961.

(18) Jafari Behbahani, T.; Ghotbi, C.; Taghikhani, V.; Shahrabadi, A., *Fuel* **2014**, *133,* 63-72.

(19) Hamadou, R.; Khodja, M.; Kartout, M.; Jada, A., *Fuel* **2008**, *87,* 2178-2185.

(20) Sim, S. K.; Okatsu, K.; Takabayashi, K.; Fisher, D. B.; Sim, S. K.; Okatsu, K.; Takabayashi, K.; Fisher, D. B., *Asphaltene-Induced Formation Damage: Effect of Asphaltene Particle Size and Core Permeability*. 2013.

(21) Bagherzadeh, H.; Rashtchian, D.; Ghazanfari, M. H.; Kharrat, R., *Energy Sources, Part A: Recovery, Utilization, and Environmental Effects* **2014**, *36,* 1077-1092.

(22) Jafari Behbahani, T.; Ghotbi, C.; Taghikhani, V.; Shahrabadi, A., *Oil & Gas Science and Technology-Rev. IFP Energies nouvelles* **2015**, *70,* 1051-1074.

(23) Dong, Z.-x.; Wang, J.; Liu, G.; Lin, M.-q.; Li, M.-y., *Petroleum Science* **2014**, *11,* 174-180.

(24) Lawal, K. A.; Crawshaw, J. P.; Boek, E. S.; Vesovic, V., *Energy & Fuels* **2012**, *26,* 2145-2153.

(25) Boek, E. S.; Ladva, H. K.; Crawshaw, J. P.; Padding, J. T., *Energy & Fuels* **2008**,

22, 805-813.

(26) Boek, E. S.; Wilson, A. D.; Padding, J. T.; Headen, T. F.; Crawshaw, J. P., *Energy & Fuels* **2009**, *24,* 2361-2368.

(27) Gon, S.; Fouchard, D. M., *Energy & Fuels* **2016**, *30,* 3687-3692.

(28) Papadimitriou, N. I.; Romanos, G. E.; Charalambopoulou, G. C.; Kainourgiakis, M. E.; Katsaros, F. K.; Stubos, A. K., *Journal of Petroleum Science and Engineering* **2007**, *57,* 281-293.

(29) Mikami, Y.; Liang, Y.; Matsuoka, T.; Boek, E. S., *Energy & Fuels* **2013**, *27,* 1838-1845.

(30) Hung, J.; Castillo, J.; Reyes, A., *Energy & Fuels* **2005**, *19,* 898-904.

(31) Seifried, C. M.; Crawshaw, J.; Boek, E. S., *Energy & Fuels* **2013**, *27,* 1865-1872.

(32) Zanganeh, P.; Ayatollahi, S.; Alamdari, A.; Zolghadr, A.; Dashti, H.; Kord, S., *Energy & Fuels* **2012**, *26,* 1412-1419.

(33) Zanganeh, P.; Dashti, H.; Ayatollahi, S., *Fuel* **2015**, *160,* 132-139.

(34) Mohammadi, S.; Rashidi, F.; Mousavi-Dehghani, S. A.; Ghazanfari, M.-H., *The Canadian Journal of Chemical Engineering* **2016**, *94,* 1820-1829.

(35) Li, X.; Fan, H.; Fan, X., *Chemical Engineering Science* **2015**, *137,* 458-465.

(36) Li, X.; Fan, X., *International Journal of Greenhouse Gas Control* **2015**, *36,* 106-113.

(37) Farokhpoor, R.; Bjørkvik, B. J. A.; Lindeberg, E.; Torsæter, O., *International Journal of Greenhouse Gas Control* **2013**, *12,* 18-25.

(38) Saraji, S.; Goual, L.; Piri, M.; Plancher, H., *Langmuir* **2013**, *29,* 6856-6866.

(39) Hildebrand, J. H.; Scott, R. L., *The Solubility of Noneletrolytes*. 3rd ed.; Reinhold Publishing: New York, 1950.

(40) Buckley, J. S.; Wang, J. X., *J. Pet. Sci. Eng* **2002**, *33,* 195.

(41) Wang, J.; Buckley, J. S., *Energy & Fuels* **2003**, *17,* 1445-1451.

(42) Wang, J. X.; Buckley, J. S., *Energy & Fuels* **2001**, *15,* 1004-1012.

(43) Weitz, D. A.; Huang, J. S.; Lin, M. Y.; Sung, J., *Physical Review Letters* **1985**, *54,* 1416-1419.

(44) Yudin, I. K.; Nikolaenko, G. L.; Kosov, V. I.; Agayan, V. A.; Anisimov, M. A.; Sengers, J. V., *International Journal of Thermophysics* **1997**, *18,* 1237-1248.

(45) Yudin, I. K.; Nikolaenko, G. L.; Gorodetskii, E. E.; Kosov, V. I.; Melikyan, V. R.; Markhashov, E. L.; Frot, D.; Briolant, Y., *Journal of Petroleum Science and Engineering* **1998**, *20,* 297-301.

(46) Ashoori, S.; Abedini, A.; Saboorian, H.; Nasheghi, K. Q.; Abedini, R., *Journal of the Japan Petroleum Institute* **2009**, *52,* 283-287.

(47) Mullins, O. C.; Sheu, E. Y.; Hammami, A.; Marshall, A., *Asphaltenes, Heavy Oils, and Petroleomics*. Springer: New York, 2007.

(48) Ghanavati, M.; Shojaei, M.-J.; S. A, A. R., *Energy & Fuels* **2013**, *27,* 7217-7232.

(49) Ilyin, S.; Arinina, M.; Polyakova, M.; Bondarenko, G.; Konstantinov, I.; Kulichikhin, V.; Malkin, A., *Journal of Petroleum Science and Engineering* **2016**, *147,* 211-217.

(50) Maqbool, T.; Srikiratiwong, P.; Fogler, H. S., *Energy & Fuels* **2011**, *25,* 694-700.

(51) Alfi, M.; Banerjee, D.; Nasrabadi, H., *Energy & Fuels* **2016**, *30,* 8962-8967.

(52) Alfi, M.; Nasrabadi, H.; Banerjee, D., *Fluid Phase Equilibria* **2016**, *423,* 25-33.

(53) Luo, S.; Lutkenhaus, J. L.; Nasrabadi, H., *Langmuir* **2016**, *32,* 11506-11513.